Correlation between machining direction, cutter geometry and step-over distance in 3-axis milling: Application to milling by zones.

Johanna Senatore, Stéphane Segonds, Walter Rubio, Gilles Dessein

Correlation between machining direction, cutter geometry and step-over distance in 3-axis milling: Application to milling by zones

Johanna Senatore [a], Stéphane Segonds [a], Walter Rubio [a,*], Gilles Dessein [b]

[a] *Institut Clément Ader, Toulouse, France*
[b] *Laboratoire de Génie de Production, Tarbes, France*

Keywords:
3-axis machining
Effective radius
Tool choice
Free-form surface
Machining zones

A B S T R A C T

Computer-Aided Manufacturing (CAM) occupies an increasingly important role in engineering with all it has to offer in terms of new possibilities and improving designer/manufacturer productivity. The present study addresses machining of free-form surfaces on a 3-axis NC machine tool. There have recently been a large number of studies devoted to planning tool paths on free-form surfaces with various strategies being adopted. These strategies are intended to increase efficiency by reducing the overall length of machining. Often, the choice of the cutter is arbitrary and the work focuses on planning. In order to boost productivity, the present work offers assistance in choosing the cutting tool, the machining direction and cutting by surface zones, adopting a milling strategy by parallel planes. To do so, a comparison is made between milling using a spherical end milling cutter and a torus end milling cutter with the same outer radius. This comparison relates to the radius of curvature of the trace left by the cutter at the point of contact between the tool and the workpiece in relation to the direction of feed motion.

1. Introduction

Free-form parts have become a regular feature of our daily lives. These harmonious shapes answer to criteria of style or are of a functional nature and require an ever higher level of quality. Moulds and dies are examples of parts that are mainly made up from free-form surfaces. They require good surface conditions and extremely reduced shape defects.

Machining moulds or dies is a long and costly process. Considering the time needed for finishing and polishing operations for free-form surfaces it can be seen that the latter can represent a considerable part of the overall machining time. One of the goals with automatic path generation is to obtain planning that will tend to minimise finishing and polishing operations over the entire surface while maintaining reasonable productivity.

Until now, methods for automatic generation of paths as currently used have included milling using guide surfaces [1], parallel plane milling [2] and iso-parametric milling [3]. Parallel plane milling has the advantage of generating paths that do not overlap, which limits the appearance of non-machined areas. But this strategy is not optimal in terms of cutter paths and scallop height. For example, if you mill a work-piece with considerable variations from the normal, you will see a contraction of the successive passes due to the need to respect the scallop height. The loss of time and thus of productivity arises from poor control over the scallop height along the paths: only the maximum scallop height produced is known [4]. This observation led to the notion of "generation of paths with constant scallop height".

A considerable number of works have been devoted to calculating the scallop height within the scope of free-form surfaces. Warkentin et al. [5] stated the problem for a spherical end milling cutter, [6] addressed the issue for a flat end milling cutter tilted by an angle in the direction of milling, and [7] concentrated on torus end milling cutters for 5-axis machining. These studies were conducted in an algebraic manner from simplified hypotheses: constant curvature, approximated cutter geometry and planar studies. Using such approximations within the framework of algebraic methods leads some authors to implement numerical methods for scallop height calculation [8]. For a spherical end milling cutter, various methods [9–12] have been studied to work from each point of a path and then compute the position of the points for the following path and so respect an imposed scallop height.

Another idea developed in the literature that also uses numerical resolution is that involving the "swept surface" [13

* Correspondence to: Institut Clément Ader, Université Paul Sabatier, 118 route de Narbonne, F-31062 Toulouse, France. Tel.: +33 561558824.
E-mail addresses: rubio@cict.fr, walter.rubio@univ-tlse3.fr (W. Rubio).

whose centre moves on the path of the CL cutter location points. However, finding the surface envelope generated by a torus end milling cutter is a much more awkward problem. In [14,15], a calculation method is adopted to give an approximation of the surface swept by the cutter during 5-axis machining with a torus mill.

Several types of milling cutters are currently used in 3-axis milling: spherical end cutters, flat end or torus end cutters. The commonest choice is the spherical end cutter and a number of research works have been conducted into the choice of dimensions for such a tool. Thus, Lo [16] presents an extremely widely used method to address milling using a spherical end milling cutter: firstly a cutter whose diameter is as large as possible is used to remove as much material as possible. The cutter leaves un-machined areas behind it that correspond to zones of local interference. A tool whose diameter is defined in relation to the curvature of the un-machined zones is then used. The criterion of choice for the large diameter tool is based on minimisation of the "overall length of the paths covered by the two cutters". Lai et al. [17] propose a different approach suited to pocket machining and sizes the large cutter in relation to the minimum dimension of the pocket. Meanwhile, Vickers and Quan [6] addresses the comparison of flat end or spherical end milling cutters in relation to the effective radii of the tools. This study was only conducted for the case of milling a plane surface. In the studies concerned, the choice of cutter (often spherical) is only stated to eliminate collisions. In the article by Lasemi et al. [18], it is clearly stated that the choice of cutter in 3-axis machining of free-form surfaces is only calculated to avoid local interference between the tool and the surface. The cutter choice (geometry and size) for convex surfaces is never proposed as all types can be used. This is clearly a shortcoming as when you analyse the performance of CAM programs various strategies are implemented with no accompanying assistance in the choice of cutter. Taking a look, for example, at the possibilities for milling a surface in 3 axes on a Catia V5R19 or Topsolid, various strategies are on offer but the choice of cutter and the machining direction are left for the user to decide on.

Often the studies presented focus on a single tool geometry. Reducing machining time on a 3-axis machine involves diminishing the overall path to be covered while respecting a maximum scallop height. When the toolpath is made up of small, line segments, the milling time is not proportional to the distance covered [19], but a reduction of the overall length will allow for shorter machining time. To reduce the length of milling, the distance between the passes must be as big as possible to reduce their number. With this aim, a series of works was based on initial tool paths in the direction of the largest slope [20–23]. The authors show that such paths can quickly lead to looping between successive passes. To avoid this, they mill by zones, eliminating loops. Working from a first path, the following paths are calculated to respect the scallop height. The next paths gradually deviate and lose their orientation along the steepest slope. The machining strategy's validity becomes questionable as the step-over distance ceases to be optimal. The purpose of the present work is neither to seek to determine locally an optimum direction at a given point nor a maximum permissible scallop height but rather to contribute a global improved solution using an indicator λ. λ represents the ratio between the step-over distance of a torus cutter and the step-over distance of a spherical cutter.

The present article focuses on the choice of milling cutters and the machining directions to be favoured in 3-axis machining of a free-form surface using a strategy of parallel planes. The method for choosing the cutter is not based on local sizing for it to be outside interference in the concave areas of the workpiece. Where the cutter chosen cannot reach all the areas of the workpiece to be machined due to problems of interference, those left behind will then be reworked by smaller-sized cutters [24]. The method described allows the cutter geometry to be correlated with the milling directions by computing the radius of curvature for the trace left by the cutter at a point.

In order to generalise the study, a torus end milling cutter was chosen. A flat end mill or a spherical end milling cutter are just specific instances of the toroidal cutter.

The article is organised as follows: in Section 2, computation of the envelope curve of a cutter, computation of the effective radius and calculation of the step-over distance in relation to the cutter geometry and the surface and direction of milling are introduced. Section 3 is devoted to the study of parameters having an influence on the step-over distance. In this section, an essential relation is established in order to define the angular domain for which a torus milling cutter is more effective than a spherical cutter. The surface can be broken down into zones based on this angular domain combined with a representation of all directions of steepest slope of a surface. Applying appropriate milling directions to these zones allows machining times to be reduced considerably. Section 4 covers an application to validate the method and help in choosing the cutter. Having considered this example, the method's potential in studying machining strategies is demonstrated.

2. Envelope curve, effective radius and step-over distance

The present section proposes to compute the effective radius R_{eff} for each cutter geometry. The reasoning is pursued for a torus end milling cutter with torus radius r and cutter radius R. By extension, the effective radius R_{eff} of a flat end cutter will be determined taking $r = 0$ and that of a spherical end cutter taking $R = r$. Computation of the effective radius requires knowledge of the cutting tool envelope curve. The main stages in determining an envelope curve are recalled below.

2.1. Determining the swept curve

In this subsection, the principle of the swept curve for a torus end milling cutter on a 3-axis NC machine tool is introduced. Let $\mathbf{S}(u, v)$ be the surface to be machined. The global reference in which the surface is expressed (Fig. 1) is called $\Re_s(\mathbf{O}, \mathbf{x_s}, \mathbf{y_s}, \mathbf{z_s})$. The axis $\mathbf{z_s}$ of this reference is the machine spindle axis. Cutter positioning in the machine tool space is performed by programming the tool centre point denoted $\mathbf{C_L}$. For each point $\mathbf{C_C}$ of $\mathbf{S}(u, v)$, the cutter is positioned tangential to the surface $\mathbf{S}(u, v)$ through point $\mathbf{C_L}$ defined by:

$$\mathbf{OC_L} = \mathbf{OC_C} + r\mathbf{n_{CC}} + (R - r)\frac{\mathbf{z_s} \wedge (\mathbf{n_{CC}} \wedge \mathbf{z_s})}{\|\mathbf{z_s} \wedge (\mathbf{n_{CC}} \wedge \mathbf{z_s})\|} \tag{1}$$

with $\mathbf{n_{CC}}$ the normal to the surface at point $\mathbf{C_C}$.

Let $\Re_\alpha(\mathbf{C_L}, \mathbf{x_\alpha}, \mathbf{y_\alpha}, \mathbf{z_\alpha})$ be a reference such that the direction of feed motion $\mathbf{V}(\alpha)$ belongs to the plane $(\mathbf{x_\alpha}, \mathbf{z_\alpha})$.

$\mathbf{V}(\alpha)$ in $\Re_\alpha$ is defined by:

$$\mathbf{V}(\alpha) = \begin{pmatrix} 1 \\ 0 \\ a(\alpha) \end{pmatrix}_{\Re_\alpha}. \tag{2}$$

$a(\alpha)$ is calculated for the cutter to move tangentially to the surface $\mathbf{S}(u, v)$ at the point. The tangent plane is defined by $\mathbf{n_{CC}}$; this translates by:

$$\mathbf{V}(\alpha) \cdot \mathbf{n_{CC}} = 0. \tag{3}$$

As the cutter moves, it will generate a surface called the "sweep surface". This is the surface envelope for the set of successive cutter positions. The sweep surface is thus the convergence of the set of profile generators for the cutter obtained for each position.

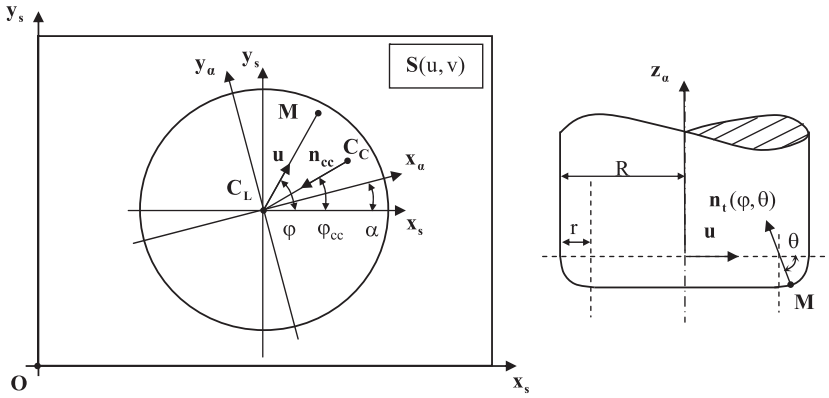

Fig. 1. Definition of parameters for positioning of the torus end milling cutter.

In order to determine the sweep curve of the cutter tool, the normal to the cutter is called $\mathbf{n_t}(\theta, \varphi)$. The set of points belonging to the cutter profile generator is defined by the following equation:

$$\mathbf{n_t}(\theta, \varphi) \cdot \mathbf{V}(\alpha) = 0. \tag{4}$$

At point $\mathbf{C_C}$, $\mathbf{n_t}(\theta, \varphi)$ is colinear with $\mathbf{n_{CC}}$ (cf. Eq. (1)). Since the point $\mathbf{C_C}$ verifies Eq. (4), it belongs to the envelope curve.

A point M of the cutting tool is defined in $\Re_\alpha$ by (Fig. 1):

$$\mathbf{C_L M} = \mathbf{T}(\theta, \varphi) = \begin{pmatrix} (R - r\,(1 - \cos\theta))\cos(\varphi - \alpha) \\ (R - r\,(1 - \cos\theta))\sin(\varphi - \alpha) \\ r\sin\theta \end{pmatrix}_{R_\alpha}$$

$$\text{with } \theta \in \left[-\frac{\pi}{2}, 0\right] \text{ and } \varphi \in [0, 2\pi]\,. \tag{5}$$

The normal to the tool in $\Re_\alpha$ is deduced:

$$\mathbf{n_t}(\theta, \varphi) = \begin{pmatrix} \cos(\varphi - \alpha)\cos\theta \\ \sin(\varphi - \alpha)\cos\theta \\ \sin\theta \end{pmatrix}_{R_\alpha}. \tag{6}$$

Whence the expression of the condition for a point to belong to the cutter profile generator:

$$\cos(\varphi - \alpha)\cos\theta + a(\alpha)\sin\theta = 0. \tag{7}$$

In what follows it will be considered that $a(\alpha) \geq 0$, corresponding to the case where the cutter has an upward movement, but the downward moving cutter can be treated in the same way.

Let angle φ_{CC} characterise the point of contact $\mathbf{C_C}$ (Fig. 1).

For $a(\alpha)$ to be positive, the direction of $\mathbf{x_\alpha}$ varies by $\pm\frac{\pi}{2}$ in relation to $\mathbf{C_L C_C}$ in the plane $(\mathbf{C_L}, \mathbf{x_s}, \mathbf{y_s})$. $\alpha \in \left[\varphi_{cc} - \frac{\pi}{2}, \frac{\pi}{2} + \varphi_{cc}\right]$ is obtained. When $\alpha = \varphi_{cc}$ the cutter moves along the steepest slope. When $\alpha = \varphi_{cc} - \frac{\pi}{2}$ or $\alpha = \frac{\pi}{2} + \varphi_{cc}$, resolution of Eq. (3) gives $a(\alpha) = 0$ representing a horizontal movement of the cutter.

Computation of the envelope curve is a function of the direction of feed motion that the cutter follows. This direction is parametrised by the angle α as previously defined. At a point of contact $\mathbf{C_C}$, for each direction $\mathbf{x_\alpha}$, the corresponding envelope curve can be defined.

Carrying over $\cos(\theta)$ and $\sin(\theta)$, resolved from Eq. (7), into Eq. (5) gives the envelope curve $\mathbf{C_e}(\varphi, \alpha)$ in reference $\Re_\alpha$:

$$\mathbf{C_e}(\varphi, \alpha) = \begin{pmatrix} \left(R - r\left(1 - \dfrac{a(\alpha)}{\sqrt{\cos^2(\varphi - \alpha) + a(\alpha)^2}}\right)\right)\cos(\varphi - \alpha) \\ \left(R - r\left(1 - \dfrac{a(\alpha)}{\sqrt{\cos^2(\varphi - \alpha) + a(\alpha)^2}}\right)\right)\sin(\varphi - \alpha) \\ \dfrac{-r\cdot\cos(\varphi - \alpha)}{\sqrt{\cos^2(\varphi - \alpha) + a(\alpha)^2}} \end{pmatrix}_{R_\alpha} \tag{8}$$

with $a(\alpha) > 0$, $\varphi \in [0, 2\pi]$ and $\alpha \in \left[\varphi_{cc} - \frac{\pi}{2}, \frac{\pi}{2} + \varphi_{cc}\right]$.

A number of envelope curves are shown on an inclined plane (30° slope) machined in different directions α (Fig. 2). With no loss in generality, in the example $\varphi_{cc} = 0$. The angle $\alpha = 0°$ corresponds to the direction with the steepest slope (up milling or down milling), the angle $\alpha = 90°$ is perpendicular to the direction of the steepest slope (horizontal machining) and an intermediate angle $\alpha = 45°$. The milling cutter chosen ($R = 5$ and $r = 2$) was modelled by its torus. The thick-lined curve represents the envelope curve. The point of contact $\mathbf{C_C}$ and the tool centre point $\mathbf{C_L}$ are also shown.

2.2. Computation of the effective radius

The effective radius of the envelope curve at point of contact $\mathbf{C_C}$ is sought. The effective radius corresponds to the radius of curvature on $\mathbf{C_C}$ of the envelope curve $\mathbf{C_e}(\varphi, \alpha)$ projected in a plane normal to the direction of feed motion along a direction parallel to the direction of feed motion.

Note $\mathbf{C_{e\_proj}}(\varphi, \alpha)$, the envelope curve $\mathbf{C_e}(\varphi, \alpha)$ projected on the plane normal to the direction of feed motion. The effective radius $R_{\text{eff}}(\varphi, \alpha)$ can be calculated as follows:

$$R_{\text{eff}}(\varphi, \alpha) = \frac{\left\| \frac{\partial \mathbf{C_{e\_proj}}(\varphi,\alpha)}{\partial \varphi} \right\|^3}{\left\| \frac{\partial \mathbf{C_{e\_proj}}(\varphi,\alpha)}{\partial \varphi} \wedge \frac{\partial^2 \mathbf{C_{e\_proj}}(\varphi,\alpha)}{\partial \varphi^2} \right\|}. \tag{9}$$

Computation of the effective radius needs to be done at point of contact $\mathbf{C_C}$, that is for the angle $\varphi = \varphi_{cc}$. Carrying over the value φ_{CC} of angle φ into the effective radius Eq. (9), the value of the effective radius at the point of contact $\mathbf{C_C}$ can be calculated, whatever the angle α. It should be noted that the effective radius of a spherical cutter is equal to R.

2.3. Step-over distance calculation

This subsection established a relation expressing step-over distance AB (cf. Fig. 3) as a function of the workpiece's geometry (ρ: radius of curvature), the cutter geometry (R_{eff}: effective radius) and the scallop height h_c. To compute this, consider a convex curve at point of contact $\mathbf{C_C}$. This curve corresponds to the intersection between the surface of the workpiece and the plane perpendicular to the direction of feed motion. In the zone studied, the radius of curvature is assumed to be constant.

In the triangles (OBC) or (OAC) and (OAB), the step-over distance AB can be calculated as follows:

$$AB = \left(\frac{h_c\,(2R_{\text{eff}} - h_c)\,(2\rho + h_c)\,(2\rho + 2R_{\text{eff}} + h_c)}{(\rho + h_c)^2}\right)^{0.5}. \tag{10}$$

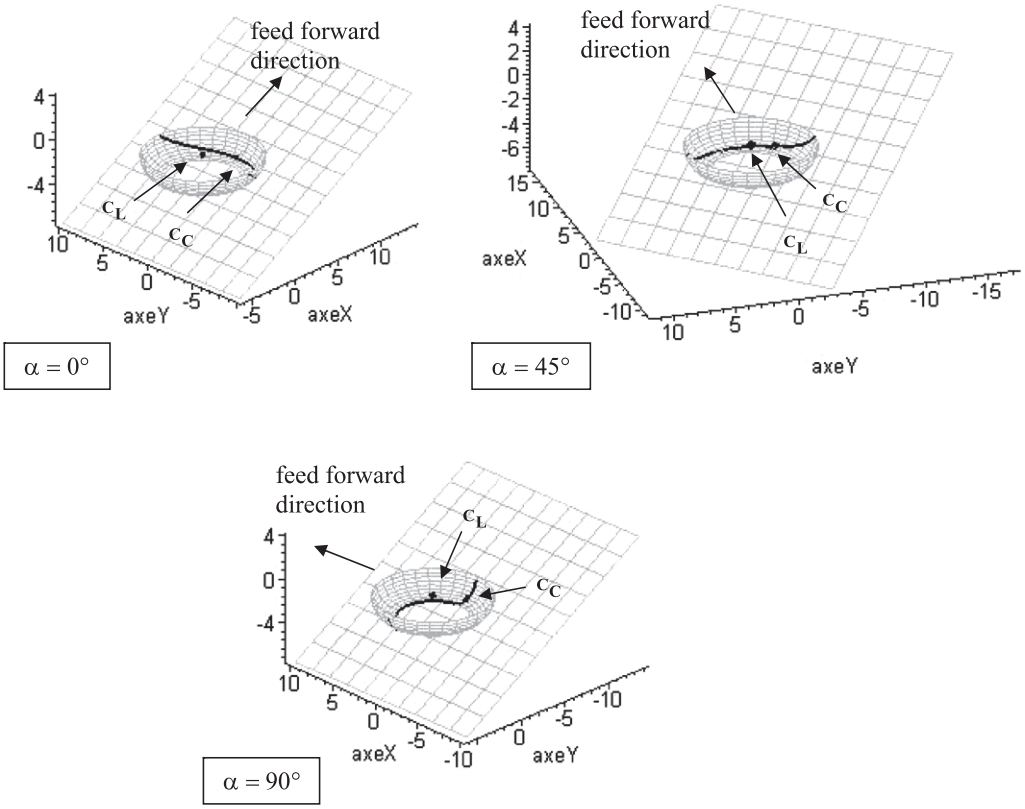

Fig. 2. Sweep curves for various angles α.

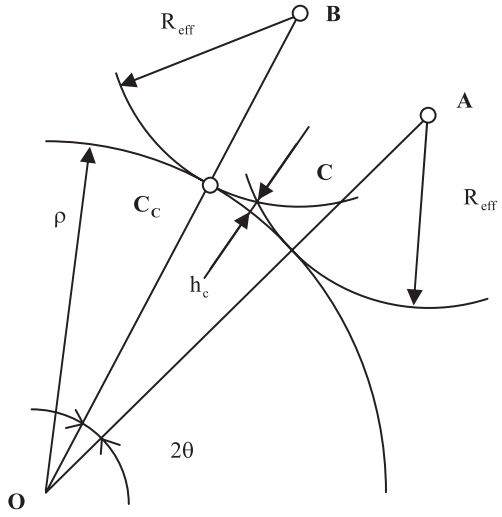

Fig. 3. Calculating step-over distance on a convex curve.

By assuming that $h_c \ll R$ and $h_c \ll \rho$, the following is obtained:

$$AB = \left(\frac{8h_c R_{\text{eff}}\,(\rho + R_{\text{eff}})}{\rho}\right)^{0.5}. \tag{11}$$

It can readily be seen from Eq. (11) that the effective radius R_{eff} is the most influential parameter for step-over distance calculation.

In order to quantify the gain on the step-over distance between a torus mill and a spherical cutter, the gain λ is defined by:

$$\lambda = \frac{\left(\frac{8h_c R_{\text{eff}}(\rho+R_{\text{eff}})}{\rho}\right)^{0.5}}{\left(\frac{8h_c R(\rho+R)}{\rho}\right)^{0.5}} = \sqrt{\frac{R_{\text{eff}}\,(\rho + R_{\text{eff}})}{R\,(\rho + R)}}. \tag{12}$$

For a plane with null curvature, it can be postulated that $\rho \gg R_{\text{eff}}$. Eq. (12) giving the gain becomes:

$$\lambda = \sqrt{\frac{R_{\text{eff}}}{R}}. \tag{13}$$

λ represents the ratio between the step-over distance of a torus cutter and the step-over distance of a spherical cutter. The torus cutter starts to become advantageous when λ is greater than 1.

3. Parameters influencing the step-over distance

Analysis of parameters having an influence on the step-over distance is intended to propose a cutter geometry appropriate to the surface to be machined and improve productivity. Many articles address the choice of the spherical end milling cutter dimensions, focusing on local interference problems (analysis of local curves). However, there is no complete study covering the choice between different cutter geometries used in 3-axis milling.

3.1. Influence of direction of feed motion α and the slope angle

Fig. 4 shows the gain λ in relation to the direction of feed motion α and the slope angle S_a of the plane surface $\mathbf{S}(u, v)$ defined as follows:

$$\mathbf{S}(u, v) = \begin{pmatrix} 100u \\ 100v \\ 100u \tan\left(\frac{\pi S_a}{180}\right) \end{pmatrix} \quad \text{with } (u, v) \in [0, 1]^2. \tag{14}$$

The milling cutter chosen is defined by $R = 5$ and $r = 2$. Whatever the slope angle S_a of the plane, the point of contact is defined at $\varphi_{CC} = 0$. The plane shown in black is gain equal to 1. The domain over which the gain is greater than 1 is dependent

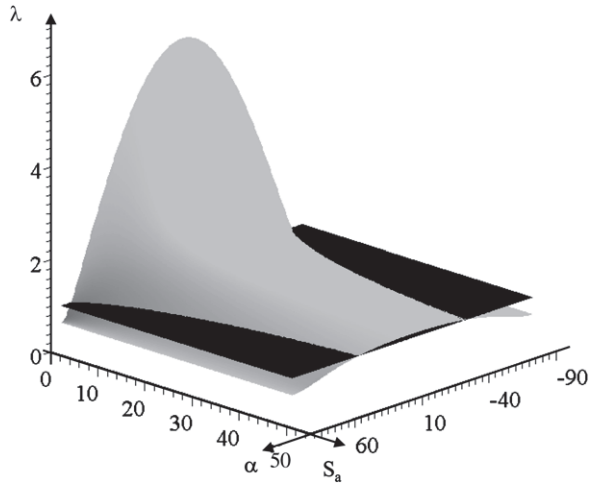

Fig. 4. Gain λ in relation to the direction of feed motion and slope angle S_a.

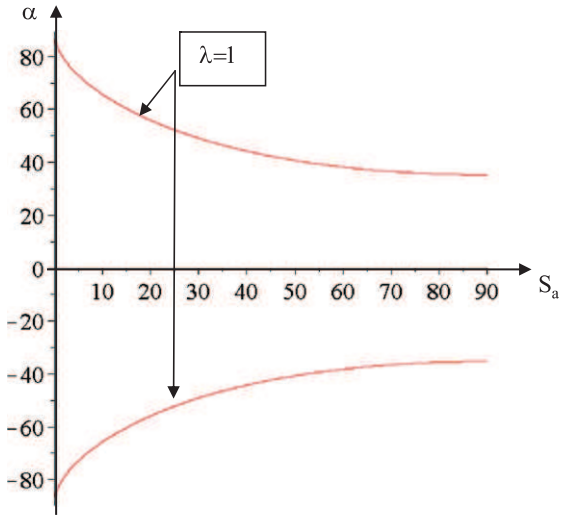

Fig. 5. Relation between direction of feed motion and slope angle.

on the slope. Over zones with a slight slope, use of a torus milling cutter will be recommended and the range for use of the direction of feed motion will be significant. However, over zones with a steep slope, use of a torus cutter can rapidly lead to having gain λ lower than 1. When the cutter advances along the steepest slope ($\alpha = 0$), the gain λ will always be greater than 1. $\lambda \geq 1$. The gain λ tends towards $\sqrt{\frac{r}{R}}$ when the direction of feed motion is horizontal. It can start to be seen from this example that for steeply sloped surfaces, use of a spherical end cutter may be preferable as the gain λ can be less than 1.

As the surface is parametrised by the angle of the slope S_a, the gain λ given by Eq. (12) is a function of the direction of feed motion α and the angle of the slope S_a. By resolving:

$$\lambda(\alpha, S_a) = 1 \tag{15}$$

the angular intervals inside which the gain λ is greater than 1 can be determined. This is translated graphically by Fig. 5.

3.2. Influence of the torus radius on the gain λ

Regardless of the cutter, a relation is sought that allows the efficiency of a torus milling cutter to be determined in relation to that of a ball-end cutter. The following equation was resolved:

$$\lambda(\alpha, S_a, r, R) = 1. \tag{16}$$

Resolution of Eq. (16) achieved using the Maple program leads to the following result:

$$\alpha = \pm a \tan\left(\frac{1}{\sqrt{\sin(S_a)\,(1+\sin(S_a))}}\right). \tag{17}$$

This result is somewhat surprising but of considerable interest as it is independent of R and r. Fig. 5 is thus valid whatever the cutter dimensions.

A relation is obtained between the slope angle S_a at the point of contact and the direction α such that $\lambda = 1$. At a point of a free-form surface, the slope angle is characterised by the angle between the cutter axis and the normal to the surface at that point. For each point of a surface, the value of α can be determined translating the fact that the step-over distance of a torus milling cutter is equal to the step-over distance of a spherical milling cutter. The closer this value comes to 90°, the more it will be advantageous to take a torus milling cutter.

Where the slope is steep, the angle α tends towards $\alpha_0 = \pm a \tan\left(\frac{1}{\sqrt{2}}\right) \approx \pm 35°$. This means that the gain λ will always be greater than 1 in an interval greater than [−35°, 35°]. This interval grows as the slope diminishes.

Using this indicator, it will be possible to identify the milling directions to be chosen to reduce the length of machining.

3.3. Determining machining zones

This result will also be used to determine machining parameters for the surface in different zones. Initially, the maximum slope denoted $S_{a\max}$ of the surface is calculated. $S_{a\max}$ can be applied in Eq. (17) to determine the angle $\alpha_{\max}$. At any point on the surface, this angle characterises an interval $I_{\max} = 2 * \alpha_{\max}$ around the direction of the steepest slope (denoted S_d), such that $\lambda \geq 1$. Any portion of the surface having an interval with variation in direction of steepest slope (denoted IS_d) less than $I_{\max}$ will have at least one machining direction that ensures that at any point $\lambda \geq 1$. Eq. (17) is fundamental. It expresses a connection between the effectiveness of a torus cutter to an interval $I_{\max}$ around the direction with the steepest slope S_d. Determining surface zones verifying $I_{\max} > IS_d$ validates the choice of a torus cutter and allows a machining direction to be determined. All these aspects are applied to an example in the following section.

4. Application to an example

The present example will show how the previous developments allow a milling direction to be chosen. Assume a Bezier surface $\mathbf{S}(u, v)$ (cf. Eq. (18)) of degree 2 × 2 defined by Fig. 6. This surface is symmetrical in relation to the plane $X = 20$:

$$\mathbf{S}(u,v) = \sum_{i=0}^{2}\sum_{j=0}^{2} B_j^2(u) B_i^2(v) \mathbf{OP_{ij}} \text{avec} (u,v) \in [0,1]^2 . \tag{18}$$

$B_j^2(u)$ and $B_j^2(u)$ are Bernstein polynomials:

$\mathbf{P_{00}} = (0, 0, 0)$, $\mathbf{P_{01}} = (20, 0, 10)$, $\mathbf{P_{02}} = (40, 0, 0)$
$\mathbf{P_{10}} = (0, 40, 5)$, $\mathbf{P_{11}} = (20, 40, 15)$, $\mathbf{P_{12}} = (40, 40, 5)$
$\mathbf{P_{20}} = (0, 80, 20)$, $\mathbf{P_{21}} = (20, 80, 35)$, $\mathbf{P_{22}} = (40, 80, 20)$.

For a set of points (cross-hatched with 640 points), Fig. 7 shows the directions of the steepest slope S_d of the surface shown above. This surface, that seems to be relatively elementary, has extremely pronounced variations in direction of the steepest slope going from 14° to 166°. For the same set of points, Fig. 8 shows the angles of slopes S_a for the surface shown in Fig. 6. For each point of the surface, the angular interval over which the gain λ is greater than

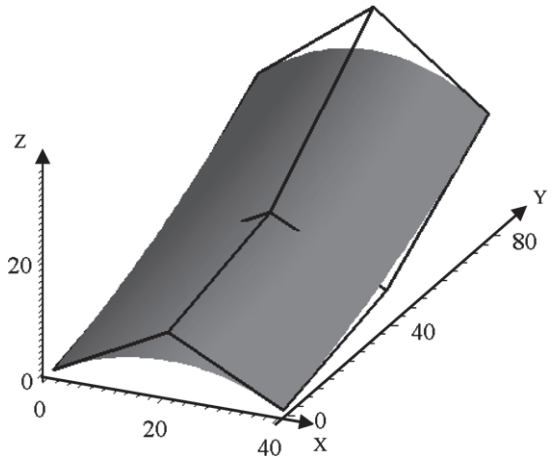

Fig. 6. Bezier surface.

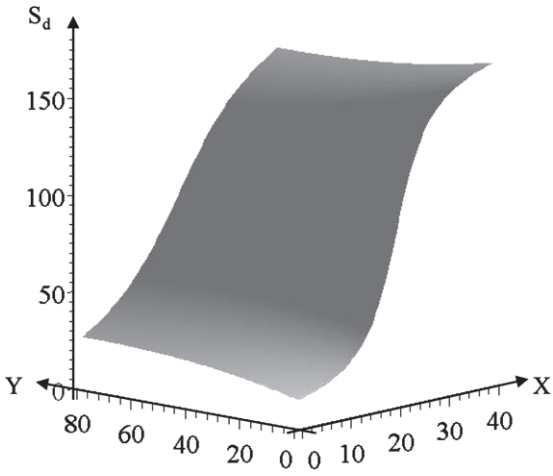

Fig. 7. Direction of steepest slope S_d.

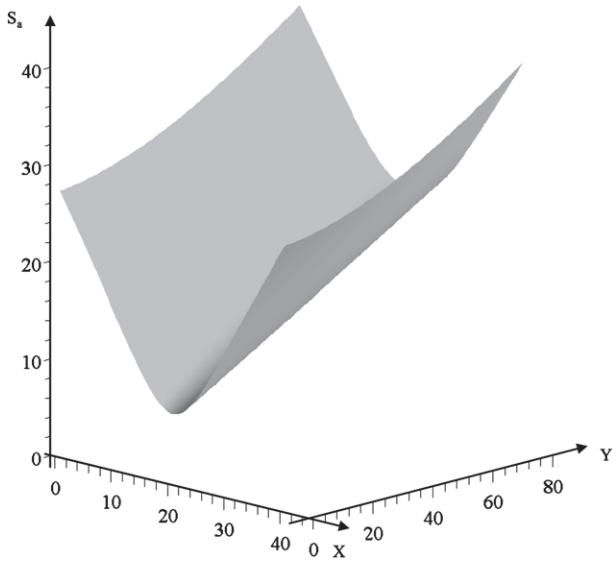

Fig. 8. Slope angles S_a.

1 is calculated. For all machining directions (between $-180°$ and 180°), Fig. 9 plots the percentage of points with gain λ greater than 1. It can be seen that initially there is the same percentage of points for all values of α_i and $\alpha_i + 180°$. This is normal as the envelope curve is identical at a point for diametrically opposed directions. It can be observed that whatever the direction of feed motion chosen, 50%–70% of points have a gain λ greater than 1. The maximum is reached for $\alpha = 0$ or $\pm 180°$. No favoured direction can be identified for the torus milling cutter to be more efficient. This result can be explained in relation to Eq. (17). In this surface $S_{a\max} = 40°$. This enables the interval $I_{\max}$ equal to 86° to be determined. Fig. 7 shows that the directions with the steepest slope S_d vary over an interval of [14°, 166°] that is on $IS_d = 152°$. As $IS_d > I_{\max}$, it is impossible to find a machining direction such that at any point $\lambda \geq 1$. Breakdown of the surfaces into zones has to be performed from Fig. 7. The surface is to be broken down such that the intervals IS_d in each zone are smaller than the intervals $I_{\max}$ for each zone. Breaking down along the planes $Y =$ constant would not be effective as the intervals IS_d in each zone would remain practically unchanged. Rather, zones need to be defined by planes $X =$ constant. The breakdown into 2 zones on $X = 20$ would lead to having for the 2 zones values for S_d of between [14°, 90°] and [90°, 166°] that is $IS_d = 76°$. The intervals $I_{\max}$ would remain at 86° as in each zone $S_{a\max} = 40°$. A situation would then obtain where for each zone $I_{\max} > IS_d$ but practically equal. The machining directions chosen would be respectively 52° ((90 + 14)/2) and 128°((90 + 166)/2). This situation leads to having points where $\lambda \approx 1$. However, choosing a torus cutter remains preferable from a cutting speed perspective, but the width between passes will be equivalent to that calculated for a spherical cutter.

It was then decided to address the problem in three surface portions. The first portion called "left lateral" (left side) goes from $X = 0$ to $X = 13$. By symmetry, the "right lateral" (right side) is considered as going from $X = 27$ to $X = 40$. The third portion, called "central" includes the surface of $X = 13$ to $X = 27$. A regular breakdown was sought without attempting to optimise the zones. This issue will be pursued further in future works. The same study as above was applied to the 3 portions of the surface. The result over the percentage of points is given in Fig. 10. Analysis of the "central" part shows that using a torus milling cutter will be truly advantageous in the interval $\alpha \in [70°, 110°]$ (modulo 180°) with 100% of points that have $\lambda > 1$. Outside this interval the percentage of points drops rapidly and can become extremely small (for the direction $\alpha = 0°$).

The two "left lateral" and "right lateral" portions are symmetrical in relation to the direction $\alpha = 0°$. For the "left lateral" portion, the interval having 100% of points with $\lambda > 1$ is located for $\alpha \in [10°, 60°]$ (modulo 180°). However, some directions are to be totally rejected as no point (or extremely few of them) has $\lambda > 1$ (between 110° and 150°). For the "right lateral" portion, the interval with 100% of points is located between $\alpha \in [120°, 170°]$ (modulo 180°). As for the "left lateral" portion, some directions are to be totally proscribed (between 30° and 70°). It can be seen that intervals that are advantageous for some zones are intervals to be proscribed for others.

In order to confirm the method's usefulness, the overall length covered by the centre of the cutter was calculated for different strategies. First of all, a strategy involving parallel planes along 3 directions (0°, 45° and 90°) using 5 different cutters was applied to the entire surface. The maximum scallop height between 2 passes was 0.01 mm. The lengths covered in the different cases are given in Table 1.

Arbitrary choices of cutter and machining direction can lead to a considerable increase in machining lengths. The results from Fig. 10 can then be applied taking a direction with $\lambda > 1$ for each of the elementary surfaces (left lateral, right lateral and central). The "left lateral", "central" and "right lateral" surfaces are respectively milled in the directions at 45°, 90° and 135°. The directions for each zone are chosen in the interval where $\lambda > 1$. As for the breakdown into zones, work to optimise the direction is now to be pursued. The lengths covered are given in Table 2. This example

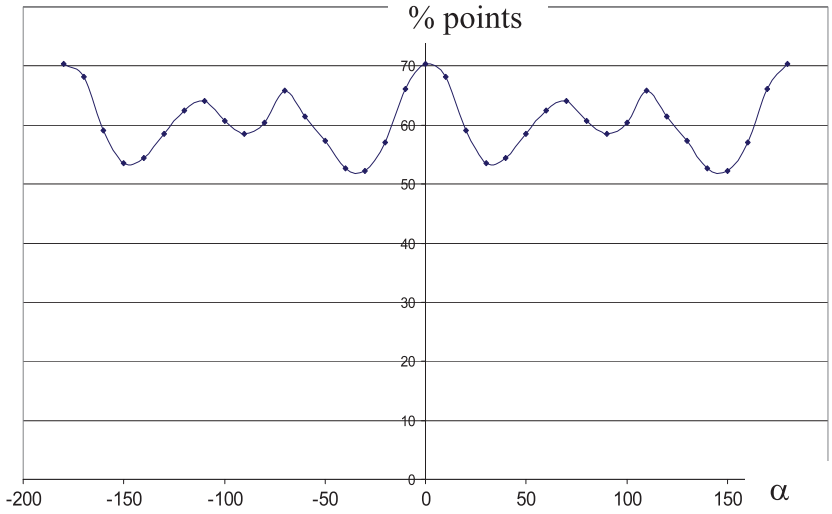

Fig. 9. Percentage of points with $\lambda > 1$.

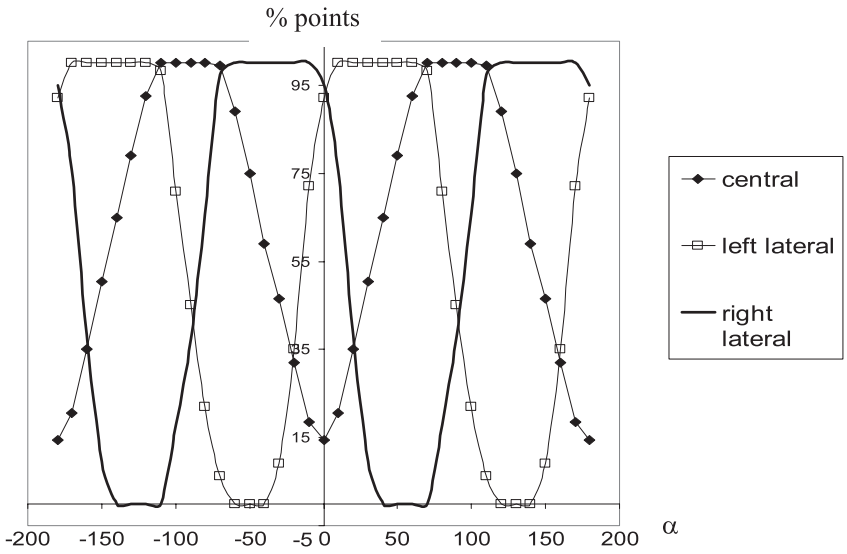

Fig. 10. Percentage of points with $\lambda > 1$ for 3 parts of the surface.

Table 1
Machining lengths with any cutter and direction for the entire surface.

	Direction 0° (mm)	Direction 45° (mm)	Direction 90° (mm)
Cutter $R = 5\ r = 5$	6 173	6 808	6310
Cutter $R = 5\ r = 4$	7 005	7 420	6243
Cutter $R = 5\ r = 3$	8 237	8 260	6334
Cutter $R = 5\ r = 2$	10 247	9 937	6636
Cutter $R = 5\ r = 1$	14 712	13 758	7084

Table 2
Machining length with privileged directions for the partitioned surface.

	Left lateral (45°) (mm)	Central (90°) (mm)	Right lateral (135°) (mm)	Total (mm)
$R = 5\ r = 5$	2086	2018	2086	6190
$R = 5\ r = 4$	1950	1935	1950	5835
$R = 5\ r = 3$	1839	1835	1839	5513
$R = 5\ r = 2$	1745	1830	1745	5320
$R = 5\ r = 1$	1666	1746	1666	5078

shows that study of the gain λ offers advantages in helping to choose a cutter and a milling direction. In the above example, the machining lengths vary from 14 712 mm (arbitrary choice) to 5 078 mm (privileged choice). Table 2 shows that choosing a torus milling cutter ($R = 5, r = 1$) associated with appropriate machining directions allows for savings of 18% as compared with a ball-end cutter on this workpiece.

In order to validate the method concretely, two workpieces were milled (Fig. 11) using the same cutter (torus milling cutter with 4 teeth $R = 5$ and $r = 2$ Fig. 12) and applying the strategy by 3 zones (45°, 90° and 135°) and the strategy in a single zone with a milling direction at 0°. Each region is milled under a parallel planes strategy following the recommended machining direction. The chosen cutting speed was 470 m/min (with spindle rotation speed of 15,000 r.p.m.) and feed rate of 1200 mm/min. Table 3 summarises the calculated lengths, the milling times measured and the gains obtained:

The time-saving is extremely close to the gains in lengths and confirms the method's advantage in concrete terms.

A roughness meter was used to perform 6 measurements per workpiece in the zones identified on Fig. 13. The results are given in Table 4.

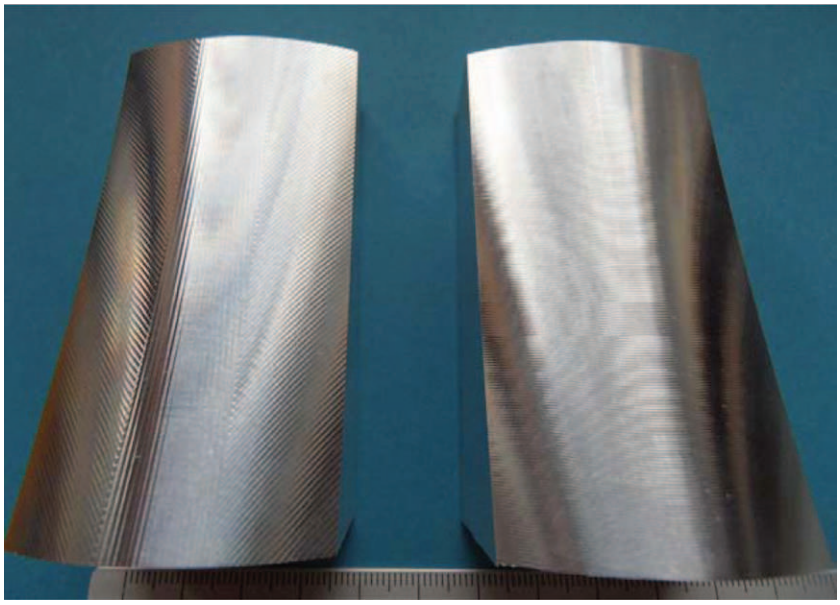

Fig. 11. Bezier surfaces machined.

Table 3
Comparison between the 2 machining strategies.

	Single zone (0°)		3 zones		Gain	
	Length	Real time	Length	Real time	Length	Real time
Cutter $R = 5$ $r = 2$	10 247 mm	10 min 5 s	5320 mm	5 min 32 s	48%	45%

Fig. 12. Torus milling cutter ($R = 5$ $r = 2$).

Table 4
Roughness measurements on 2 workpieces.

	Entire surface		Partitioned surface	
	Ra (μm)	Rt (μm)	Ra (μm)	Rt (μm)
Measurement n°1	1.28	6.1	1.08	6.15
Measurement n°2	1.91	8.64	1.38	7.83
Measurement n°3	2.2	8.9	1.44	8.94
Measurement n°4	0.64	3.93	1.82	8.69
Measurement n°5	0.41	2.66	1.2	6.49
Measurement n°6	0.49	3.05	1.25	7.84

Two roughness profiles were shown in Figs. 14 and 15 corresponding to measurement n°2 of the entire surface and measurement n°5 of the partitioned surface. The scallop height profiles are clearly represented. For the same length of evaluation (4 mm), different profiles can be seen leading, for the partitioned surface, to a greater step-over distance than that for the entire surface. For the entire surface, maximum roughness is obtained in the central part of the workpiece. Measurements n°4, n°5 and n°6

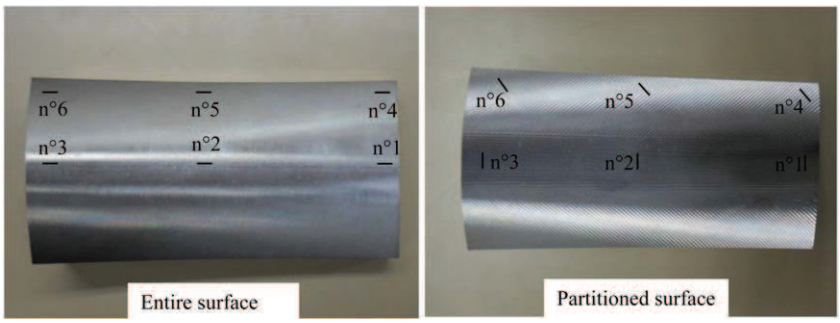

Fig. 13. Locations of roughness measurements on the 2 workpieces.

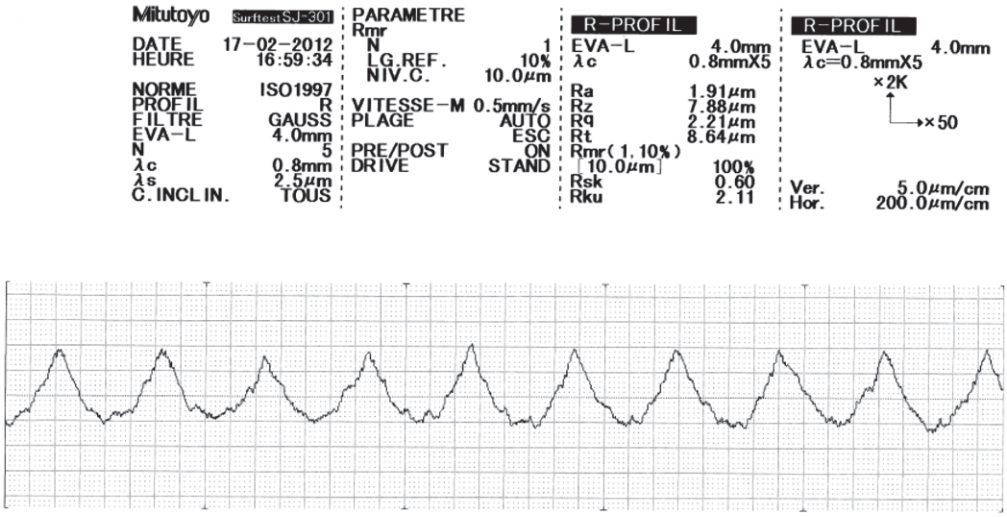

Fig. 14. Measurement n°2 of the entire surface.

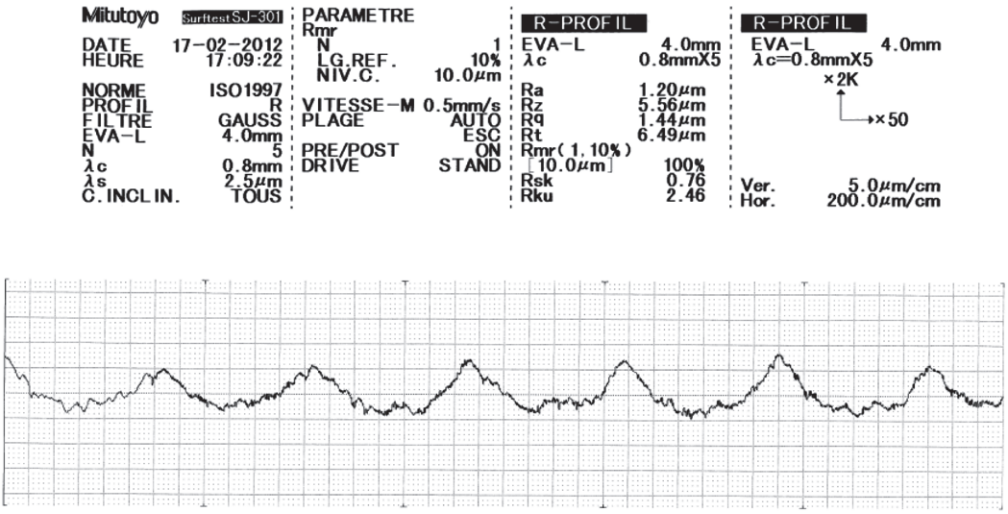

Fig. 15. Measurement n°5 of the partitioned surface.

show profiles with very low scallop heights. For the partitioned surface, the breakdown enabled a more regular scallop height to be obtained close to the maximum authorised value (h max $=$ 0.01 mm) over the entire workpiece. The above study shows that choosing a torus milling cutter is appropriate when milling by zones.

Conclusion

An indicator was sought to assist in making the best choice of milling cutter. Many works relate to the strategies to be applied (iso-parametric, parallel planes iso-scallop) for milling of free-form surfaces. In these various strategies, the initial set-up, first tool paths and cutters are often imposed from the start. For the parallel plane strategy, the present inquiry focused on offering help in choosing the appropriate cutters for end milling of free-form surfaces. For the purposes of the study, it was assumed that the surfaces are machinable at any point without interference. With this concern to select a tool, the effective radius of a torus milling cutter was calculated. The effective radius was computed by the radius of curvature of the envelope curve projected onto a plane perpendicular to the direction of feed motion. Thus, the effective radius and the step-over distance were calculated, at any point, for any direction of feed motion. A relation was established enabling the angular interval for which the step-over distance of a torus mill is greater than the step-over distance of a spherical mill to be determined. Using this interval and the representation of directions with the steepest slope, it can be readily determined whether the surface needs to be broken down into a number of zones. Such a breakdown is then performed in order to reduce the intervals of variation of the steepest slope in each zone. This means that for any point, the milling directions to be chosen for a torus milling cutter to be more productive than a spherical cutter can be determined.

An example was taken showing that when the surface is milled in totality, it is not essential to choose a torus milling cutter. Furthermore, no feed rate directions to be favoured emerge. The surface was then divided up (arbitrarily into 3 parts). Application of the method shows clearly that a torus milling cutter proves to be the best choice for the 3 zones but that different directions are to be favoured for each surface. This study opens up interesting perspectives in planning tool paths for the milling of free-form surfaces. It provides an indicator to assist in choosing the appropriate cutters and the preferred machining directions and also in how to break down a surface into a number of zones. These works open up a range of perspectives to reduce machining time by optimising machining zones and associated directions.

References

[1] Kim BH, Choi BK. Guide surface based tool path generation in 3-axis milling: an extension of the guide plane method. Computer-Aided Design 2000;32: 191–9.

[2] Huang Y, Oliver JH. Non constant parameter NC toolpath generation of sculptured surfaces. International Journal of Advanced Manufacturing Technology 1994;9:281–90.

[3] Looney G, Ozsoy T. NC machining of free form surfaces. Computer-Aided Design 1987;19:85–90.

[4] Kim BH, Choi BK. Machining efficiency comparison direction-parallel tool path with contour parallel tool path. Computer-Aided Design 2002;34:89–95.

[5] Warkentin A, Bedi S, Ismail F. 5-axis milling of spherical surfaces. International Journal of Machine Tools and Manufacture 1996;36:229–43.

[6] Vickers GW, Quan KW. Ball-mills versus end-mills for curved surface machining. ASME Journal of Engineering for Industry 1989;111:22–6.

[7] Wang XC, Yu Y. An approach to interference-free cutter position for five-axis free-form surface side finishing milling. Journal of Materials Processing Technology 2002;123:191–6.

[8] Redonnet JM. Etude globale du positionnement d'un outil pour l'usinage de surfaces gauches sur machines cinq axes et génération de trajectoires. Ph.D. Thesis. University Paul Sabatier, Toulouse; 1999.

[9] Suresh K, Yang DCH. Constant scallop-height machining of free-form surfaces. ASME Journal of Engineering for Industry 1994;116:253–9.

[10] Lin RS, Koren Y. Efficient tool-path planning for machining free-form surfaces. ASME Journal of Engineering for Industry 1996;118:20–8.

[11] Sarma R, Dutta D. The geometry and generation of NC tool paths. Journal of Mechanical Design 1997;119:253–8.

[12] Yoon JH. Fast tool path generation by the iso-scallop height method for ball-end milling of sculptured surfaces. International Journal of Production Research 2005;43:4989–98.

[13] Peternell M, Pottman H, Steiner T, Zhao H. Swept volumes. Computer-Aided Design and Applications 2005;2:599–608.

[14] Roth D, Bedi S, Ismail F, Mann S. Surface swept by a toroidal cutter during 5-axis machining. Computer Aided Design 2000;33:57–63.

[15] Mann S, Bedi S. Generalization of the imprint method to general surfaces of revolution for NC machining. Computer-Aided Design 2002;34:373–8.

[16] Lo CC. Two-stage cutter-path scheduling for ball-end milling of concave and wall-bounded surfaces. Computer-Aided Design 2000;32:597–603.

[17] Lai W, Faddis T, Sorem R. Incremental algorithms for finding the offset distance and minimum passage width in a pocket machining tool path using the Voronoï technique. Journal of Materials Processing Technology 2000;100: 30–5.

[18] Lasemi A, Xue D, Gu P. Recent development in CNC machining of free-form surfaces: a state-of-the-art review. Computer Aided Design 2010;52:641–54.

[19] Pessoles X, Landon Y, Rubio W. Kinematic modelling of a 3-axis NC machine tool in linear and circular interpolation. International Journal of Advanced Manufacturing Technology 2010;47:639–55.

[20] Maeng HY, Ly MH, Vickers GW. Feature based machining of curved surfaces using the steepest directed tree approach. Journal of Manufacturing Systems 1996;15:379–91.

[21] Chen ZC, Song D. A practical approach to generating accurate iso-cusped tool paths for three axis CNC Milling of sculptured surface parts. Journal of Manufacturing Processes 2006;8:29–38.

[22] Chen ZC, Fu Q. A practical approach to generating steepest ascent tool paths for three axis finish milling of compound NURBS surfaces. Computer-Aided Design 2007;39:964–74.

[23] Chen ZC, Vickers GW, Dong Z. Integrated steepest-directed and iso-cusped toolpath generation for three axis CNC machining of sculptured parts. Journal of Manufacturing Systems 2003;22:190–201.

[24] Flutter A, Todd J. A machining strategy for toolmaking. Computer-Aided Design 2001;33:1009–22.